JOURNAL OF CATALYSIS 88, 65–72 (1984)

Structure and Activity of NiO/α-Al_2O_3 and NiO/ZrO_2 Calcined at High Temperatures

II. Activity in the Fuel-Rich Oxidation of Methane

G. R. GAVALAS,* C. PHICHITKUL,* AND G. E. VOECKS†

Division of Chemistry and Chemical Engineering and †Jet Propulsion Laboratory, California Institute of Technology, Pasadena, California 91125

Received December 13, 1982; revised February 14,1984

The activity of NiO/α-Al_2O_3 and NiO/ZrO_2 in the fuel-rich oxidation of methane was measured as a function of time-on-stream for different initial calcination temperatures and for different reduction–reoxidation treatments. The activity was found to decrease substantially with increasing temperature of calcination. However, the activity of the calcined catalysts increased sharply following reduction in H_2 prior to reaction. The changes in total activity are discussed in terms of changes in surface area and specific activity, the latter being the dominant factor. The change in specific activity is discussed in terms of changes in the content of excess oxygen.

INTRODUCTION

The present paper reports results on the activity of supported nickel catalysts whose chemical and physical structure were investigated in the preceding paper (Part I). The test reaction employed in the activity measurements was the fuel-rich oxidation of methane. One objective of these experiments was to relate activity to surface area and nature of the nickel species. The structure of the catalyst was varied by varying the temperature of calcination and by subjecting the catalyst to successive cycles of reduction and reoxidation.

EXPERIMENTAL

1. Materials. The samples used in the activity measurements were obtained from the same batches as the samples examined in Part I. Tables 1 and 2 list the metal and total surface areas of the samples tested.

The reaction mixture contained CH_4 (Linde, 99.997% purity), O_2 (Amweld, 99.95% purity), with diluent N_2 (Linde, 99.996% purity). The mixture was further purified by passing it through a bed of dehydrated 13X molecular sieve.

2. Equipment and analytical. Figure 1 shows a schematic of the experimental system. The reactor consisted of an alumina tube, 0.47-cm i.d. and 45-cm long heated by two independently controlled heating sections (furnaces) of 15 and 30 cm length, rated at 500 and 1000 W. The temperature was measured by a movable axial Chromel–Alumel thermocouple surrounded by a 0.15-cm quartz thermowell located at the reactor axis. The packing consisted of 10–100 mg of catalyst diluted with low surface area α-Al_2O_3 to reduce the heat release per unit volume. To achieve isothermal operation and obtain uniform velocity profile, packings of 5 cm length of low surface area α-Al_2O_3 were placed before and after the catalyst bed. The reactor was operated in a differential mode with CH_4 conversion of 2% or less. The temperature variations along and across the catalyst bed were always within ±2°C. On this basis, the reactor could be considered isothermal. Pressure was in all cases slightly above atmospheric.

The product gases were passed through a drierite column and the dry gases were analyzed by an HP 5830A gas chromatograph

0021-9517/84 $3.00

TABLE 1

Surface Areas of Zirconia-Supported Catalysts

Catalyst	S_T (m^2/g)	$S_T - S_A$ (m^2/g)
NiO/ZrO_2 noncalcined	0.93	0.54
NiO/ZrO_2-750	0.85	0.46
NiO/ZrO_2-850	0.68	0.29
NiO/ZrO_2-950	0.80	0.41
NiO/ZrO_2-1050	0.61	0.22
ZrO_2 (Norton SZ5464)	0.39	—

Note. S_T: total surface area, S_A: surface area of support.

TABLE 2

Rate Parameters of Catalysts and Supports

Catalyst	E (kcal/mol)	α	β
NiO/ZrO_2-750	23.6		
NiO/ZrO_2-850	21.0		
NiO/ZrO_2-950	21.7		
NiO/ZrO_2-1050	53.3		
NiO/α-Al_2O_3-750	28.2	0.43[a]	0.43[a]
NiO/α-Al_2O_3-850	29.3		
NiO/α-Al_2O_3-950	26.1		
NiO/α-Al_2O_3-1050	52.4		
ZrO_2	36.7		
α-Al_2O_3	35.9		

[a] At 600°C.

with a 10-foot Carbosieve (100/120 mesh) column and a thermal conductivity detector. The carrier gas was He (99.997% purity). Using temperature programming from room temperature to 150°C (30°C/min) allowed the separation of all components: O_2, N_2, CO, CO_2, H_2 CH_4. Certified gases (Scotty) were used for calibrating the gas chromatograph.

3. *Experimental procedure and data reduction.* A run was started by heating the reactor to the desired temperature under flow of nitrogen. Flow was then switched to the reacting mixture and chromatographic analyses were conducted every 10 min. A typical run lasted 5 h or longer allowing the measurement of the activity as a function of time-on-stream. In some runs the catalyst was subjected to periodic reduction–reoxidation treatments. Reduction was carried out by flowing hydrogen for 1 h at 600 to 650°C. Reoxidation was effected simply by resuming flow of the reactant mixture, following which the activity was measured for another period of about 5 h.

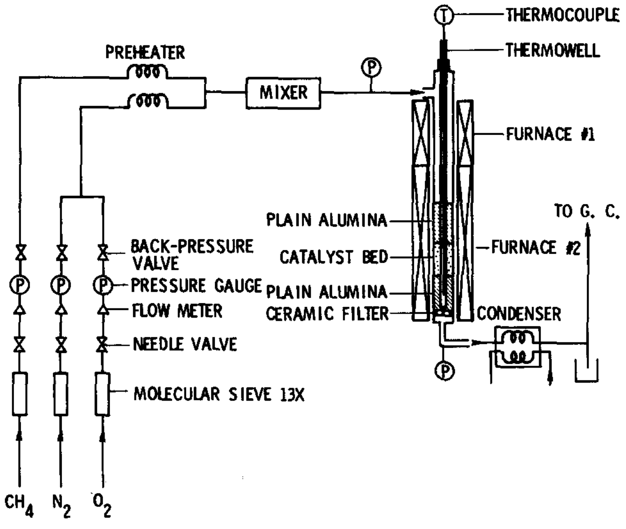

FIG. 1. Microreactor for fuel-rich oxidation of methane.

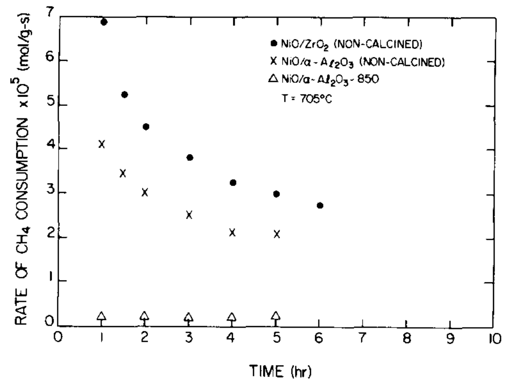

FIG. 2. Activity of noncalcined and calcined catalysts vs time-on-stream.

Preliminary tests showed that the extent of gas phase reaction and reaction at the reactor wall were negligible. From the analytical criteria reviewed by Mears (*1*), the reaction rates were free of mass and heat transfer effects. Since the conversion was kept below 2%, the rate of methane consumption was calculated from

$$r = \frac{F}{W}X$$

where F is the flow rate of methane in moles per second, W is the catalyst loading in g, and X is the fractional conversion of methane.

RESULTS AND DISCUSSION

1. *Catalytic Activity*

Figure 2 shows the activity of the noncalcined NiO/ZrO$_2$ and NiO/Al$_2$O$_3$ catalysts and of the NiO/Al$_2$O$_3$-850 catalyst versus time on stream. The activity of the noncalcined catalysts declines rapidly during the first few hours and more slowly thereafter. By contrast, the catalyst that has been calcined at 850°C displays a much lower activity which, however, remains constant with time.

Figures 3 and 4 present the activities of zirconia-supported and alumina-supported catalysts calcined at different temperatures. The reaction rates of the catalysts that have been calcined at 950 and 1050°C were corrected by subtracting the contribution of the supports. The activities are seen to decrease dramatically with calcination temperature. The activation energies derived from the Arrhenius plots are listed in Table 2. The catalysts calcined below 950°C have very similar activation energies. The variation of activity with calcination temperature is evidently due to variation in the A-factor. The calculated activation energies of the catalysts calcined at 1050°C are much higher than those corresponding to the lower calcination temperatures. These high values are probably an artifact of calcula-

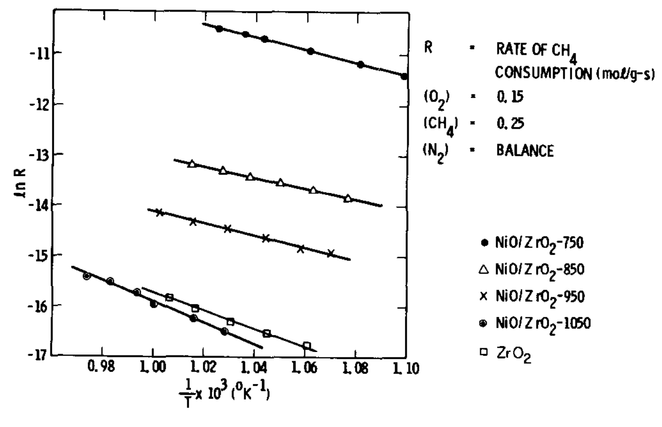

FIG. 3. Arrhenius plots for zirconia-supported catalysts.

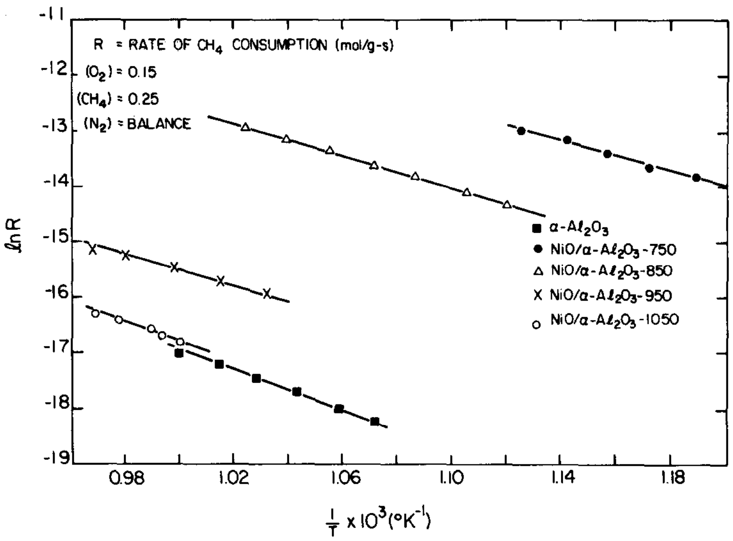

FIG. 4. Arrhenius plots for alumina-supported catalysts.

ting the specific activity by subtracting the activity of the support from the total activity. Since the support contributes roughly half of the total activity of the NiO/ZrO_2-1050 and NiO/Al_2O_3-1050, the calculation of the oxide activity by difference is subject to considerable error.

Table 2 also lists the reaction order with respect to methane and oxygen for the NiO/Al_2O_3-750 catalyst, based on the empirical rate expression

$$r = k\,[CH_4]^{\alpha}\,[O_2]^{\beta}$$

The reaction order with respect to CH_4 was obtained by varying the mole fraction of CH_4 from 0.1 to 0.4 while keeping the mole fraction of oxygen at 0.15. The order with respect to O_2 was obtained by varying the mole fraction of O_2 from 0.1 to 0.35 while keeping the mole fraction of methane at 0.25.

To interpret the variations of catalytic activity we first inquire about the state of the surface under reaction conditions. The small conversion of methane, about 2%, implies that the system CH_4–O_2–Ni does not reach equilibrium. Thus the state of the surface is determined by the competition of oxidation and reduction reactions. We will tentatively assume that the surface is maintained in the oxide form under reaction conditions.

The next question concerns the large variation of activity with calcination temperature. The rates presented in Figs. 3 and 4 are given per unit weight of the catalyst (support plus nickel oxide). To calculate the specific rates, i.e., the rates per unit surface area requires determining the surface area of nickel oxide. This cannot be readily related to the metal surface area given in Table 5 of Part I because of the redispersion accompanying reduction. However, upper and lower bounds for the oxide surface area S_{NiO} can be easily obtained in terms of the surface area of the support S_A and the total surface area S_T. If S_I is the interfacial area between oxide and support, $S_T = S_{NiO} + S_A - S_I$ or $S_{NiO} = S_T + S_I - S_A$ from which $S_T - S_A < S_{NiO} < S_T$. Table 1 shows that the oxide surface area varies by at most a factor of 4 over the range of calcination temperatures while the activity, shown in Fig. 3, varies by several orders of magnitude over the same range. Thus the variation of catalytic activity is dominated by the variation in the specific activity of nickel oxide caused by calcination. Although the areas of nickel oxide in the alumina-supported catalysts are not available, they are expected to have suffered comparable loss of oxide area during calcination. The loss of catalytic activity must be again attributed to the decrease of specific activity accompanying calcination.

The large changes of specific activity with calcination temperature may be related to the color changes listed in Tables 3 and 4 of Part I. While the noncalcined catalysts were all black, the calcined zirconia-supported catalysts were gray to gray–yellow and the calcined alumina-supported catalysts were gray to greenish. Inspection of used catalysts shows that the color of the noncalcined catalysts changes from black to grayish black with time-on-stream, whereas that of the calcined catalysts remains the same. While changes in color may be due to several phenomena, the change from black to gray has been attributed in the literature to a decrease in the concentration of excess oxygen in the bulk and the surface of the oxide upon calcination (*2–5*). The excess oxygen is in turn related to the concentration of N_i^{3+} ions by

$$\tfrac{1}{2}O_2(g) + 2Ni^{2+} = O^{2-} + 2Ni^{3+} + Ni[\,]$$

where Ni[ ] is a cation vacancy. Thus, two lattice Ni^{3+} ions are formed for each excess oxygen ion, although this relationship becomes less accurate at the surface because of the possibility of O^- as well as O^{2-} ions (*2*).

Several studies (*6–10*) have interpreted the catalytic properties of NiO in terms of its semiconductivity which can be modified by introducing altervalent cations or excess oxygen. Being a *p*-type semiconductor, NiO has electrical conductivity that increases with the concentration of Ni^{3+} ions, or excess oxygen ions. Hauffe *et al.* (*7*) and Winter (*8*) have shown that the activity of lithium-doped NiO in the decomposition of N_2O increases with conductivity, and hence, with the concentration of excess oxygen ions. Krauss (*6*) has shown that the activity of NiO in the oxidation of NH_3 to N_2O is proportional to the amount of excess oxygen in the lattice. Taking these prior facts into account, as well as the color changes with calcination, it appears quite plausible that the main parameter that determines the surface activity of NiO in methane oxidation is excess oxygen or concentration of Ni^{3+} cations.

The gradual activity decline of the noncalcined catalysts and the constant activity of the calcined catalyst observed in Fig. 2 can be explained by a slow loss of surface area or by a loss of excess oxygen. The latter explanation is consistent with the observed color changes of catalysts that have been subjected to reaction conditions. However, the former explanation is more in line with the results of the experiments reported below.

2. *Effect of Reduction*

To explore the variation of catalytic activity further, rate measurements were made after reduction of the catalysts in hydrogen. Although most nickel is converted to metal during reduction, it is quite likely that it is reoxidized upon exposure to the reactant mixture. Figure 5 shows the activities of zirconia-supported and alumina-supported catalysts before and after reduction at 650°C for 1 h. Although the activities of the two zirconia-supported catalysts differed greatly because of different calcination temperatures, the activities after reduction are essentially equal and comparable to that of the noncalcined catalyst (Fig. 2). These results suggest that upon reduction and exposure to the reactant mixture the catalyst reverts to the state of the noncalcined catalyst. Figure 5 also compares the alumina-supported catalysts before and after reduction. The activity of the NiO/α-Al$_2$O$_3$-850 and NiO/α-Al$_2$O$_3$-1050 catalysts increases by 1 and 3 orders of magnitude, respectively. The activity level after reduction is somewhat different in the two catalysts and lower than the activity of the noncalcined catalyst. These differences

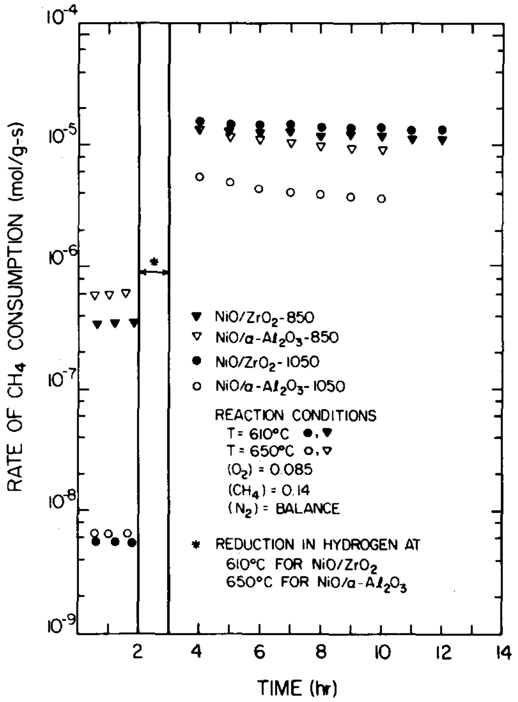

FIG. 5. Activity of various catalysts before and after reduction.

may be due to the irreversible formation of some nickel aluminate during calcination.

The sharp activity increase following reduction observed in Fig. 5 is succeeded by a gradual decline that is hardly perceptible in the logarithmic scale of the figures. To explore this activity decline further, rate measurements were carried out following a second and third successive reductions (Fig. 6). The activity increase following these latter reductions was modest since it started from a much higher level. After each reduction the activity declined gradually with time-on-stream. The activity increment after each reduction decreased slightly with each additional cycle.

Figure 7 shows the results of an experiment identical to that of Fig. 6 except for the duration of the third reduction which was 3 h rather than 1 h. The increase in the reduction time led to considerably lower activity increment than was observed in the first two reductions. It appears that the slow irreversible deactivation observed from cycle to cycle continues even in the presence of hydrogen.

The activity of nickel oxide for different reduction temperatures is shown in Fig. 8. The reaction temperature in each case is equal to the reduction temperature. The adverse effect on activity of reduction temperature predominates over the temperature dependence of the reaction rate so that the overall rate declines with increasing reduction temperature. The activity decline in all these cases is consistent with a de-

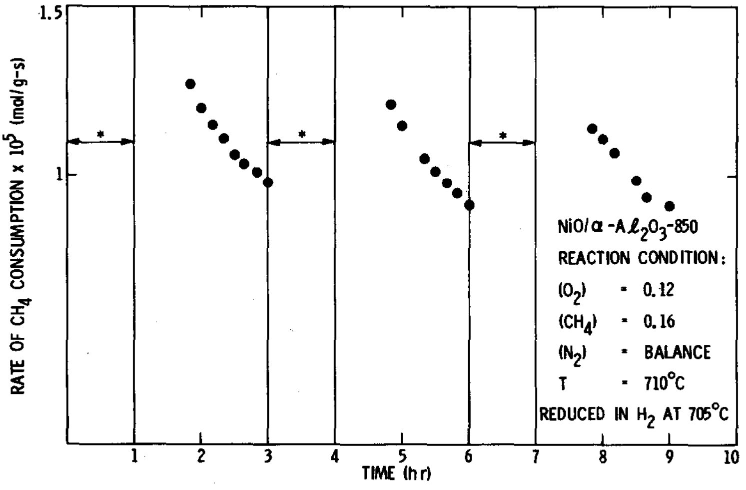

FIG. 6. Activity of alumina-supported nickel oxide subjected to a sequence of reductions.

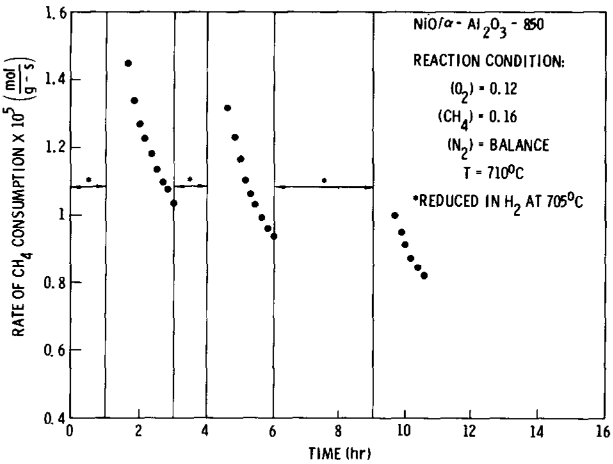

FIG. 7. Activity of alumina-supported nickel oxide subjected to reductions of different duration.

cline in surface area proceeding during reduction and during subsequent reaction.

The effect of the oxygen-to-methane ratio on the rate of activity decline is shown in Fig. 9. At 710°C the rate of activity decline appears to be independent of the O_2/CH_4 ratio in the range 0.2 to 1.2. It is important to note that up to this point CO_2 was the only oxygenated carbon product. However, when the O_2/CH_4 ratio at the inlet was lowered to 0.11, the activity (after reduction) did not decline. Under these conditions, CO and CO_2 were formed in comparable amounts. This shift in reaction products was attributed by one of the authors (Ref. (*11*), Chap. 2) to the reduction of nickel oxide to metallic nickel owing to the complete conversion of oxygen. Such complete conversion was possible in the present experiment because of the lower

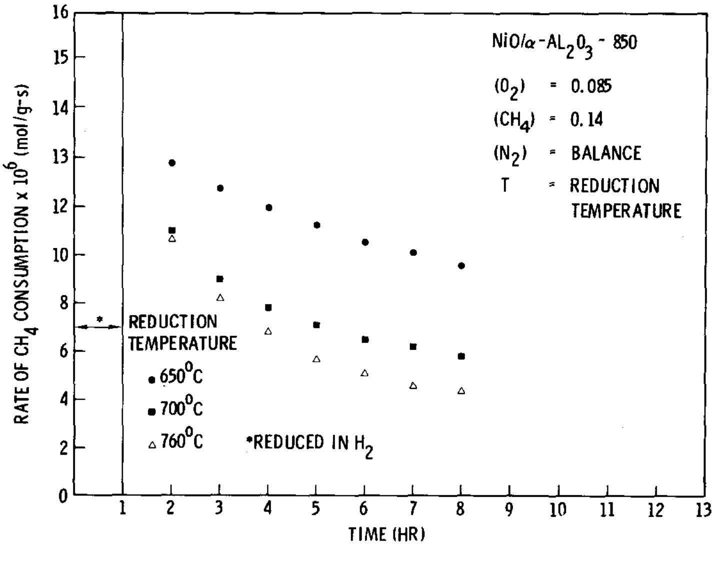

FIG. 8. Effect of reduction temperature on the activity of alumina-supported nickel oxide.

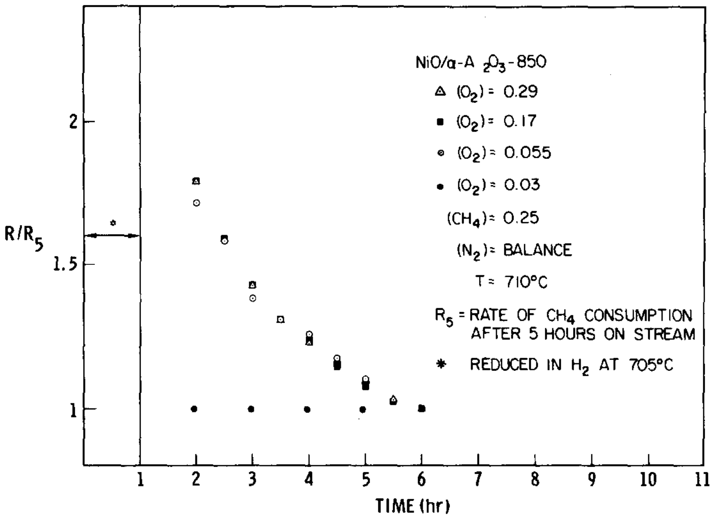

FIG. 9. Effect of partial oxygen pressure on the deactivation of alumina-supported nickel oxide.

mole fraction of oxygen introduced and the higher reaction rate observed. On the other hand, the stability of the reaction rate with time-on-stream is at variance with the results of Fig. 7 which implied loss of activity during prolonged exposure to hydrogen, conditions under which nickel was also in the form of the metal.

SUMMARY AND CONCLUSIONS

The following are the principal conclusions from the experimental results:

1. The specific activity of supported nickel oxide decreases sharply with calcination temperature but can be restored by reduction in hydrogen followed by reoxidation under reaction conditions. These variations of activity could be explained by corresponding changes in the concentration of Ni^{3+} or excess oxygen on the surface.

2. The activity of calcined catalysts remains constant with time-on-stream. The activity of noncalcined catalysts or catalysts that have been reduced and reoxidized suffer a slow decline with time-on-stream. The activity gain following reduction is diminished with higher reduction temperatures and longer reduction times.

3. The conclusions in 1 and 2 are based on the assumption that under reaction conditions the nickel is in the oxide form. This issue needs further investigation taking also into account the stabilization of activity and the shift in the reaction products observed when the oxygen to methane ratio was reduced below 0.11.

REFERENCES

1. Mears, D. E., *Ind. Eng. Chem. Proc. Des. Dev.* **10,** 541 (1971).
2. Deren', J., and Stoch, J., *J. Catal.* **18,** 249 (1970).
3. Tourky, A. R., Hanafi, Z., and Salem, T. M., *Z. Phys. Chem. (Leipzig)* **243,** 145 (1970).
4. Bielan'ski, A., Deren', J., and Wolter, M., *Kinet. Katal.* **5,** 849 (1964).
5. Krylov, O. V., "Catalysis by Nonmetals," p. 66. Academic Press, New York, 1970.
6. Krauss, W., *Z. Elektrochem.* **53,** 320 (1948).
7. Hauffe, K., Glang, R., and Engell, H. J., *Z. Phys. Chem. (Leipzig)* 201, 223 (1952).
8. Winter, E. R. S., *Discuss. Faraday Soc.* **28,** 183 (1959).
9. Parravano, G., *J. Amer. Chem. Soc.* **75,** 1452 (1952).
10. Schwab, G. M., and Block, J., *Z. Phys. Chem. (Frankfurt)* **1,** 42 (1954).
11. Phichitkul, C., "Catalytic Activity and Deactivation Mechanisms of Supported NiO in CH_4 Oxidation," Ph.D. thesis, California Institute of Technology, 1981.